MOLECULAR IMAGING AND BIOLOGY

Mol Imaging Biol (2019) 21:1157–1164
DOI: 10.1007/s11307-019-01332-7

Published Online: 8 March 2019

WMIS World Molecular Imaging Society

Check for updates

RESEARCH ARTICLE

Preoperative Differentiation of Uterine Sarcoma from Leiomyoma: Comparison of Three Models Based on Different Segmentation Volumes Using Radiomics

Huihui Xie, Xiaodong Zhang, Shuai Ma, Yi Liu, Xiaoying Wang

Department of Radiology, Peking University First Hospital, No. 8, Xishiku Street, Xicheng District, Beijing, 100034, China

Abstract

Purpose: To investigate the impact of applying three different volume of interests (VOIs) in ADC map-based radiomic analysis and compare their diagnostic performance in the differentiation of uterine sarcoma and atypical leiomyoma.

Procedures: Seventy-eight patients (29 uterine sarcomas, 49 uterine leiomyomas) imaged with pelvic magnetic resonance imaging (MRI) prior to surgery were included in this retrospective study. Manually, segmentations of VOIs covered three different regions on apparent diffusion coefficient (ADC) maps: (1) tumor, (2) tumor and small piece of surrounded tissue, and (3) whole uterus. Texture and non-texture features were extracted from each VOI. The 0.623 + bootstrap method and the area under the receiver-operating characteristic curve (AUC) were used to select the features. Twenty logistic regression models (orders of 1–20) based on different combination of image features were built for each way of image segmentation.

Results: For the first VOI region, model 18 with 18 features yielded the highest AUC of 0.830, sensitivity of 76.0 %, specificity of 73.2 %, and accuracy of 73.9 %. For the second VOI region, model 17 with 17 features yielded the highest AUC of 0.853, sensitivity of 75.5 %, specificity of 75.5 %, and accuracy of 76.8 %. For the third VOI region, model 20 with 20 features yielded the highest AUC of 0.876, sensitivity of 76.3 %, specificity of 84.5 %, and accuracy of 82.4 %.

Conclusions: Radiomic model based on features extracted from VOI that covered the whole uterus had the best diagnostic performance. Adopting VOI contained more image information that was useful in improving diagnostic performance of radiomic model.

Key words: Image segmentation, Volume of interest, Leiomyoma, Sarcoma, Uterus, Radiomics

Introduction

Uterine sarcoma was characterized by its aggressive behavior, with a great tendency of local recurrence and distant metastasis [1–3]. The preoperative differentiation of uterine sarcoma and atypical leiomyoma is crucial because many minimally/non-invasive methods that take place in the management of leiomyoma may allow uterine sarcoma being unrecognized [4]. In 2014, the US FDA issued a statement discouraging the use of power morcellation for hysterectomy and myomectomy owing to the potential for dissemination of an occult uterine sarcoma [5]. Diffusion-weighted imaging (DWI) is a powerful method that permits the quantitative evaluation of tumor tissues by displaying water molecule mobility. Apparent diffusion coefficient

Correspondence to: Xiaoying Wang; *e-mail:* cjr.wangxiaoying@vip.163.com

(ADC) values, measured *via* DWI, have shown promising results in distinguishing malignancies from benign gynecological tumors [6, 7]. Although absolute ADC values are affected by many factors and may vary between magnetic resonance imaging (MRI) systems and field strengths, histogram analyses of ADC maps may provide a more reliable assessment because the distribution parameters are independent of signal intensity [8].

Radiomics represents a process designed to extract quantitative data from radiologic images, then by building appropriate models with refined features through profound analysis of image data for diagnostic, prognostic, and predictive purpose [9–11]. Multiple studies have showed the feasibility of radiomics across imaging modalities in oncology and its effectiveness in differentiating tumors which are difficult to classify in traditional radiologic image interpretation [12–16]. Tissue characterization was one of the earliest applications in radiomic analysis [17, 18]. Lakhman et al. had investigated the feasibility of texture analysis in distinguishing leiomyosarcoma from atypical leiomyoma [19]. Given the nature of radiomics, the radiomics approach in the differentiation of uterine sarcoma and atypical leiomyoma is applicable to many types of medical images, ADC maps included.

Radiomic analysis begins with the choice of an imaging protocol, the volume of interest (VOI), and a prediction target [9]. Segmentation of VOI is the most important way in radiomic analysis. It determines which voxels within an image are analyzed [9]. Usually, VOI contains either the whole tumor or subregions (habitats). It can also be placed on metastatic lesions as well as in normal tissues [9, 11, 20]. It is well accepted that VOI should contain sufficient textural information that share similar tissue characteristics [18, 21]. In 2015, Wibmer, et al. correlated whole mount pathology maps with MRI segmentation in the differentiation of non-cancerous prostate from prostate cancer [16]. However, whole mount pathology of uterine sarcoma or leiomyoma is not available in all institutions. To separate intratumor necrosis or hemorrhage from tumor parenchyma on radiological images may be difficult without correlated whole mount pathological images. What is more, in conventional image interpretation, the differentiation of uterine sarcoma and leiomyoma in MRI depends on peri-tumor appearance such as continuity of uterine endometrial cavity, peri-tumor flow voids, ill-defined tumor margin, as well as intratumor characteristics such as intratumor hemorrhage or necrosis [2, 5, 19, 22–24]. VOI contains tumor region alone that may leave essential voxels outside the region unanalyzed.

In this study, we hypothesize that if more useful information (defined by conventional image interpretation) can be extracted from images and analyzed, the diagnostic performance of radiomic model may improve. The primary objective of this study was to compare the diagnostic performance of ADC map-based radiomic models based on features extracted from three different VOIs in the differentiation of uterine sarcoma and atypical leiomyoma.

Materials and Methods

Study Population

Our institutional review board approved this retrospective study with a waiver of the requirement for patients' informed consent. We searched a database of gynecological surgeries in our institution between July 2010 and November 2016. The inclusion criteria were patients (1) were suspected of malignant uterine mass or atypical leiomyoma in their MRI reports or diagnosis on admission, (2) had histologically proven uterine sarcoma or leiomyoma, and (3) underwent preoperative multiparametric MRI (MP-MRI) in our institution. The exclusion criteria were patients (1) without pathological results, (2) had chemotherapy or radiation or invasive therapy before MP-MRI, and (3) images with severe artifacts that would inflect the interpretation.

MR Scan Protocol

As our study population consisted of patients recruited over an extended period of time, patients underwent MRI examinations using two systems: either a 3-T system (Achieva; Philips Healthcare, Best, The Netherlands) or a 1.5-T system (Signa HDxt, GE Medical System). The imaging protocol included (1) T2-weighted fast spin-echo imaging (T2WI) in the axial, coronal, and sagittal planes; (2) axial T1-weighted fast spin-echo imaging (T1WI); (3) axial DWI with reconstruction of ADC maps; and (4) dynamic contrast-enhanced (DCE) MRI. ADC maps were generated automatically from each DWI images by the MRI system software. In this study, only ADC maps were analyzed. The parameters of DWI are presented in Table 1.

Radiomic Analysis

In 2015, Vallières et al. [25] first introduced a radiomic model built from joint PET and MRI texture features using bootstrapping evaluations. In 2017 and 2018, Zhou et al. and Dong et al. adopted this method in predicting survival and molecular markers in diffuse lower-grade gliomas and sentinel lymph node metastasis in breast cancer with high sensitivity and specificity [26, 27]. In this study, similar methods were used for radiomic analysis in this study. As shown in Fig. 1, radiomic analysis contains three major steps once the prediction target and imaging protocol were settled: image segmentation, feature extraction, and modeling. The feature extraction, modeling, and statistical analyses were performed using MATLAB (R2017a).

Image Segmentation

With reference to T2WI and DWI, image segmentation was independently performed on ADC maps by two radiologists

Table 1. Parameters of DWI

		1.5 T	3.0 T
DWI	Plane	Axial	Axial
	TR/TE	4000/56 msec	4420/70 msec
	Band width	32 kHz	32 kHz
	Section thickness	5 mm	6 mm
	Intersection gap	1 mm	1 mm
	Field of view	40–32 cm	28–32 cm
	b value	800 s/mm^2	1000 s/mm^2

TR repetition time, *TE* echo time

with 5 and 7 years of experience in oncologic MRI who were blind to the pathological results (Fig. 2). VOIs were manually drawn slice by slice using MRIcron (version 1.40). Three different VOIs were performed for each patient: VOI *No*.1 covered only the lesion within the margin (Fig. 2d), VOI *No*.2 covered the lesion and surrounded tissue (1–3 mm beyond the tumor margin) (Fig. 2e), and VOI *No*.3 covered the whole uterus (Fig. 2f).

Inter-reader and Intra-reader Agreements of VOIs and Radiomic Features

The reproducibility of inter-reader and intra-reader agreements for VOIs and radiomic features was measured using 30 randomly chosen samples from each of the three data sets of different VOIs. To evaluate intra-reader agreement, reader 1 performed the VOI delineation twice within 1 week. At the same time, reader 2 performed the VOI delineation only once to assess the inter-reader agreements by comparing with the first time of reader 1. The Dice coefficient was used to determine the spatial overlap accuracy of VOIs [28]. The Dice coefficient ranged from 0 to 1, with a high value indicating better agreement. Interclass correlation coefficient (ICC) was used to assess the reproducibility of radiomic features [29]. An ICC of greater than 0.75 was considered to represent good agreement. Reader 1 accounted for the remaining samples if good agreement was achieved.

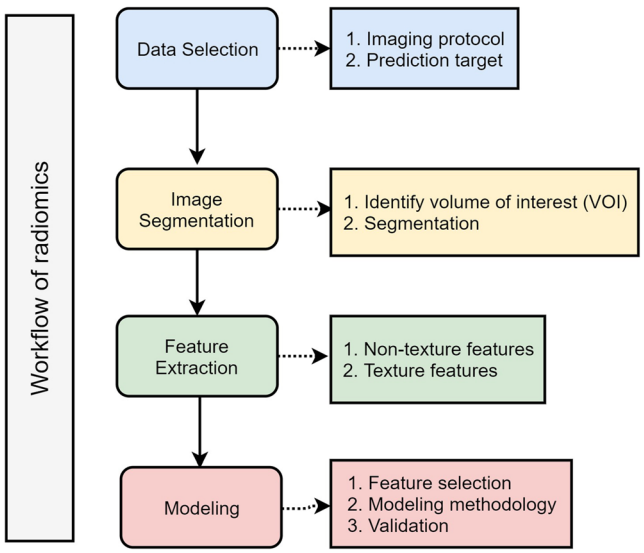

Fig. 1. Workflow of radiomics.

Feature Extraction

Figure 3 shows the procedure of radiomic feature extraction. Three extraction parameters were used: (1) 3D isotropic scale values: 0.5 mm, 1 mm, 2 mm, 3 mm, 4 mm, and 5 mm; (2) quantization algorithm: uniform and equal-probability; and (3) number of gray levels: 8, 16, 32, and 64. Three types of global features were computed using different 3D isotropic scale values. Forty types of high-order texture features were computed using the 48 possible combinations of all three extraction parameters. Four non-texture features (volume, size, solidity, and eccentricity) and 1938 texture features were extracted from each VOI eventually.

Modeling

Radiomic modeling involves three major aspects: feature reduction, feature selection, and modeling methodology. First, feature set reduction was performed using the Gain equation, based on the Spearman's rank correlation and the maximal information coefficient computed between features to obtain a reduced feature set of 50 radiomic features. After feature reduction, stepwise forward feature selection was performed for models 1 to 20 to obtain maximal 0.632 + bootstrap AUC metric. The order of model specifies the number of features chosen within the reduced feature set. Imbalanced adjusted logistic regression was utilized in the construction of binary classified radiomic model. Model's predictive performance was evaluated with average AUC, sensitivity, and specificity. Risk of uterine sarcoma was computed by the bootstrap samples for the optimal model.

Results

Patients' Characteristics

The distribution of the pathological results is shown in Table 2. Between July 2010 and November 2016, 78 patients were included in this study. Nineteen patients who had mesenchymal sarcoma and ten patients who had mixed epithelial and mesenchymal sarcoma were included in the group of uterine sarcomas. Among 49 patients who had presumed atypical leiomyoma, 8 patients had cellular leiomyoma. Among 41 patients with leiomyoma, 23 patients (56.1 %) had various degenerations. Fourteen patients (48.3 %) with uterine sarcoma underwent DWI with *b* value of 800 s/mm^2 in the 1.5-T MRI scanner. Fifteen (51.7 %) patients with uterine sarcoma and all 49 patients with uterine leiomyoma underwent DWI with *b* value of 1000 s/mm^2 in the 3.0-T MRI scanner (Table 1).

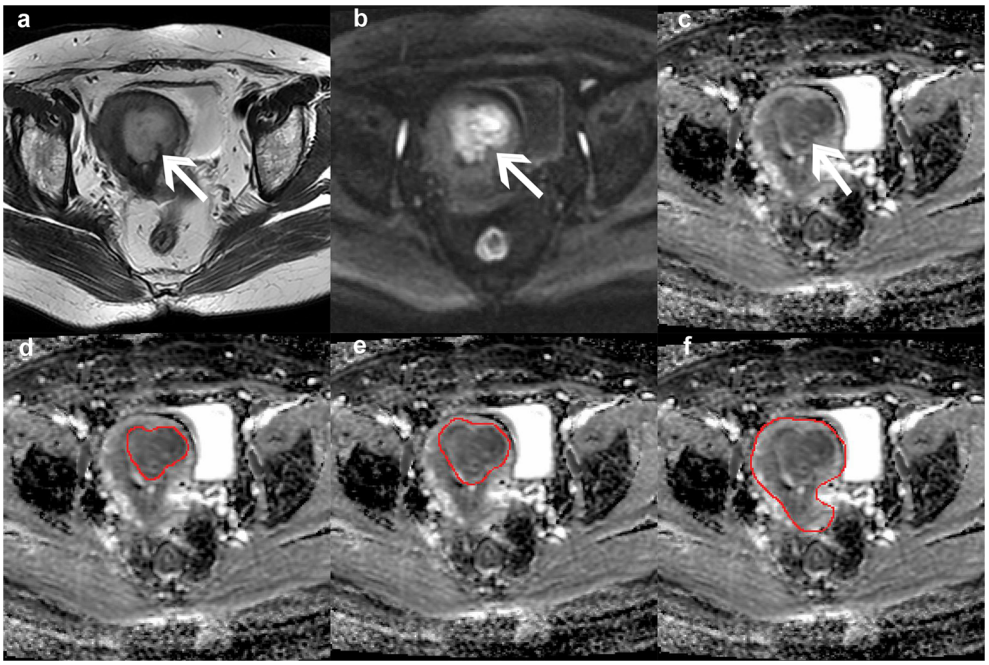

Fig. 2. Example of a 58-year-old patient with leiomyosarcoma shows image segmentation on apparent diffusion coefficient (ADC) maps with reference to axial T2-weighted imaging (T2WI) and diffusion-weighted imaging (DWI). **a** Axial T2WI, **b** DWI, and **c** ADC maps show a mass in myometrium (white arrow). **d**–**f** The segmented region of three different volume of interests (VOIs) on ADC maps. **d** VOI *No*.1 covered only the lesion, **e** VOI *No*.2 covered the lesion and surrounded tissue, and **f** VOI *No*.3 covered the whole uterus.

Inter-reader and Intra-reader Agreements of VOIs and Radiomic Features

For inter-reader agreement of VOIs, the mean Dice coefficient values were 0.923 (95 % CI, 0.910–0.933), 0.921 (95 % CI, 0.913–0.929), and 0.947 (95 % CI, 0.942–0.951) for VOI *No*.1, VOI *No*.2, and VOI *No*.3, respectively. For intra-reader agreement of VOIs, the mean Dice coefficient values were 0.920 (95 % CI, 0.910–0.930), 0.923 (95 % CI, 0.917–0.930), and 0.942 (95 % CI, 0.936–0.947) for VOI *No*.1, VOI *No*.2, and VOI *No*.3, respectively. For inter-reader agreement of radiomic features, the mean ICC values were 0.895 (95 % CI, 0.889–0.901), 0.886 (95 % CI, 0.880–0.892), and 0.889 (95 % CI, 0.882–0.895) for VOI *No*.1, VOI *No*.2, and VOI *No*.3, respectively. For intra-reader agreement of radiomic features, the mean ICC values were 0.877 (95 % CI, 0.870–0.883), 0.859 (95 % CI, 0.852–0.867), and 0.850 (95 % CI, 0.841–0.858) for VOI *No*.1, VOI *No*.2, and VOI *No*.3, respectively.

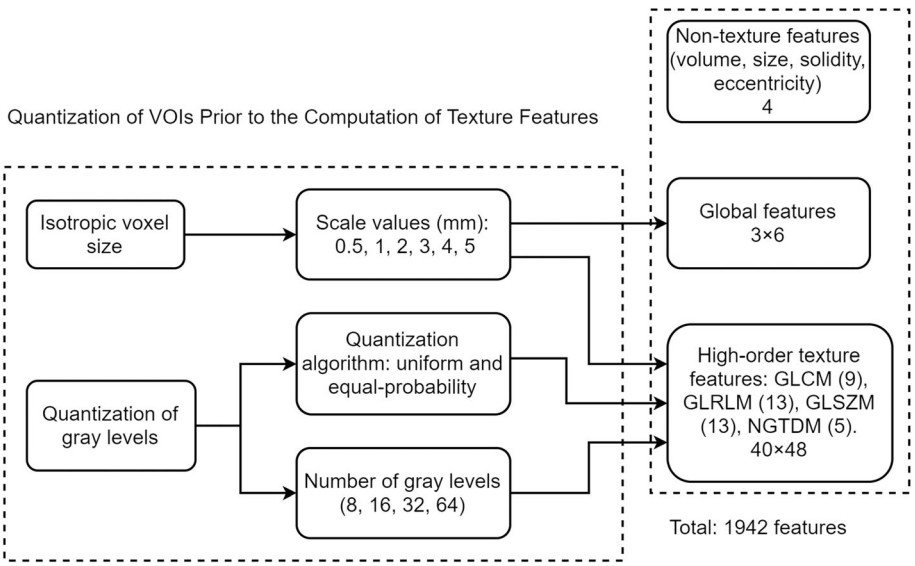

Fig. 3. Workflow of radiomic features' extraction for each volume of interst (VOI).

Table 2. Distribution of pathological results of both groups

	Uterine sarcoma ($N = 29$) Freq (%)	Uterine leiomyoma ($N = 49$) Freq (%)
Mesenchymal sarcoma		
Leiomyosarcoma	10 (34.5)	
Endometrial stromal sarcoma	5 (17.2)	
Rhabdomyosarcoma	1 (3.4)	
Undifferentiated uterine sarcoma	3 (10.3)	
Mixed epithelial and mesenchymal sarcoma		
Carcinosarcoma	7 (24.1)	
Adenosarcoma	3 (10.3)	
Coexistent leiomyomas	9 (31)	
Leiomyomas		41 (83.7)
With red degeneration		2 (4.9)
With hyaline degeneration		20 (48.8)
With hydropic changes		1 (2.4)
Cellular leiomyomas		8 (16.3)
1.5 T	14	0
3.0 T	15	49

Freq frequency

Estimation of Prediction Performance of Multivariable Models

Three feature sets extracted from VOIs of three kinds of segmentation methods underwent feature set reduction and selection. For each feature set, 1 to 20 multivariate radiomic models were constructed with combined feature that specifies the model number in which combination could reach maximal 0.632 + bootstrap AUC metric. For each feature set, the models with the best predictive performance were chosen (Fig. 4a–c). Probability of uterine sarcoma as a function of the response of the models for all the patients of the cohort was also computed (Fig. 4d–f).

Prediction Performance with Radiomic Features Extracted from VOI No.1

For the first segmentation method, model 18 with 18 features yielded the highest AUC of 0.830, sensitivity of 76.0 %, specificity of 73.2 %, and accuracy of 73.9 % (Fig. 4a). The optimal feature set included 2 histogram-based texture features (variance, kurtosis) and 16 high-order texture features (gray-level non-uniformity, zone-size non-uniformity, complexity, entropy, contrast, correlation, homogeneity, energy, variance, and dissimilarity).

Prediction Performance with Radiomic Features Extracted from VOI No.2

For the second segmentation method, model 17 with 17 features yielded the highest AUC of 0.853, sensitivity of 75.5 %, specificity of 75.5 %, and accuracy of 76.8 % (Fig. 4b). The optimal feature set included 1 non-texture feature (eccentricity), 3 histogram-based texture features (skewness), and 13 high-order texture features (gray-level non-uniformity, run-length variance, short run low gray-level emphasis, long run low gray-level emphasis, long run high gray-level emphasis, high gray-level run emphasis, low gray-level run emphasis, low gray-level zone emphasis, and small zone high gray-level emphasis).

Prediction Performance with Radiomic Features Extracted from VOI No.3

For the third segmentation method, model 20 with 20 features yielded the highest AUC of 0.876, sensitivity of 76.3 %, specificity of 84.5 %, and accuracy of 82.4 % (Fig. 4c). The optimal feature set included 1 non-texture feature (solidity), 1 histogram-based texture features (variance), and 19 textural features (gray-level non-uniformity, zone-size variance, energy, variance, entropy, and contrast).

Possibilities of All Patients Using Optimal Multivariable Models of Three VOIs

The probability of observing uterine sarcoma as a function of the response of the three multivariable models proposed in this work was calculated for all patients of the cohort (Fig. 4d–f). The probability 1 suggests uterine sarcoma, 0 suggests uterine leiomyoma with a threshold set of 0.5.

Discussion

In this study, three different VOIs were used in the extraction of radiomic features. Three optimal radiomic models were identified for the preoperative classification of uterine sarcoma and uterine leiomyoma. With the enlargement of VOI, the optimal model reached better diagnostic performance. The highest AUC reached 0.876 by radiomic features extracted from the whole uterus. VOI that covered whole uterus rather than tumor region alone was revealed to be promising for the evaluation of tumor heterogeneity and

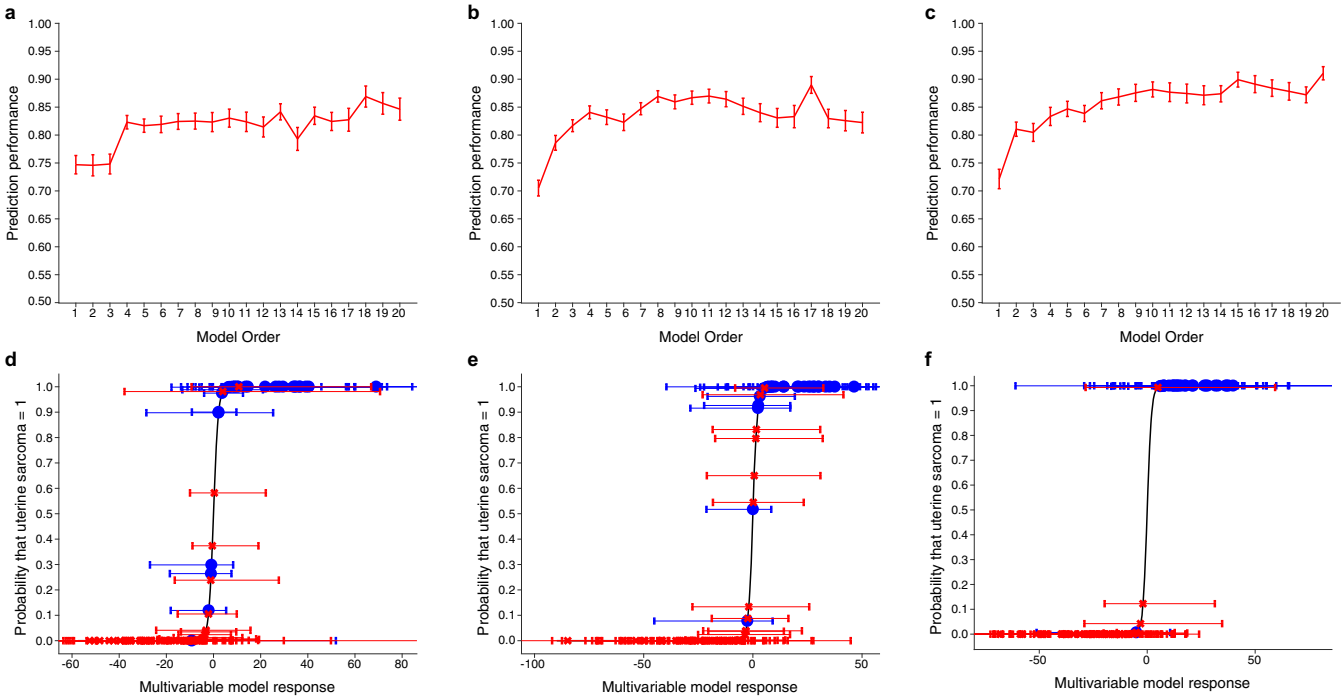

Fig. 4. Inspection of predictive properties of multivariable texture models constructed from three feature sets (**a–c**). Probability of developing uterine sarcoma as a function of the response of the multivariable model proposed in this work, for all patients of the cohort (**d–f**). The dots represent patients who had uterine sarcoma and the crosses those who had uterine leiomyoma. It can be seen that the optimal feature models can significantly separate the patients of the two pathological results for each type of volume of interest (VOI), especially in the case of VOI *No*. 3 (**f**).

provided a new option in the analysis of tumors in solid organs.

Radiomics refers to the extraction of a large array of quantitative features that evaluate gray level patterns, pixel interrelationships, and spectral patterns inside a VOI, which makes selection of an appropriate VOI the most important step. None of the previous studies had dug into the impact of choosing different VOIs and only a few had applied the whole organ delineation to perform radiomic studies. Most recently, Chen et al. had described the successful application of whole pancreas delineation (including the necrosis) in building radiomic model to predict the recurrence of acute pancreatitis [29]. Tanadini-Lang et al. analyzed the entire prostate rather than cancerous lesions within the gland and proved that texture features can predict tumor grade and aggressiveness in prostate cancer [30]. In our study, the sensitivity, specificity, accuracy, and AUC of the optimal radiomic raised with the enlargement of VOI. The possible explanation was that larger VOI not only covered the features of tumor region (*e.g.*, intratumor hemorrhage, necrosis) but also included the other predictive features outside of the tumor (*e.g.*, ill-defined tumor margin, the interrupted uterine endometrial cavity). Both Tanadini-Lang's study and our study showed that the radiomic analysis of the entire organ is a valid approach for the assessment of tumor. What is more, VOI that covered the whole uterus had the highest inter-reader and intra-reader agreements on the segmentation of VOIs. It demonstrated that the delineation of organ was less variable than the delineation of tumor with indistinct margin, which would also reduce the delineation work. These studies introduced a new method of image segmentation that might be transplant to other tumor entities. Furthermore, the automatic segmentation of uterus has been proved more accurate than manual measurement [31], which may further automatize the procedure of radiomic analysis and improve the reproducibility of radiomic models.

Features of the optimal feature set extracted from VOI *No.*1 are similar to those of VOI *No*.3, while features of the optimal feature set extracted from VOI *No*.2 are quite different. Though VOI *No*.3 contained a lot of unrelated features (*e.g.*, myometrium), redundant features can be eliminated through evaluating relevance in estimating features in the process of feature selection. The region of VOI *No*.1 and VOI *No*.2 only had little difference. It suggested that though the enlargement of VOI had brought more redundant information into analysis, it was removed through feature selection. Optimal features may vary; they suggested that uterine sarcoma was more heterogenous than atypical leiomyoma, which is in line with previous study [19]. It also illustrated that radiomics has the potential to serve as a noninvasive technique for accurate characterization of tumor microenvironment, thus improving diagnostic performance [32].

It should be noted that only ADC maps were used in this study. Axial T2WI was excluded from the radiomic analysis

because variable parameters had been used across different scanners (*e.g.*, about half of the subjects underwent axial T2WI with fat suppression). Besides, various types of degeneration or cellular subtype can cause increased intensity on T2WI for atypical leiomyoma, which was similar to the signal intensity of uterine sarcoma [7]. So, we presumed that T2WI-based radiomic features may not perform well in radiomic models. ADC values are influenced by the nuclear-to-cytoplasm ratio and cellular density in tissue; thus, this parameter varies between tumor categories [33]. Our study showed that ADC map-based radiomic features can differentiate uterine sarcoma from leiomyoma. Although Gerges et al. did not find a significant difference between leiomyoma and leiomyosarcoma from whole-lesion histogram metrics obtained on ADC maps significant [34], their study and that of Lakhman et al. found significant difference between leiomyoma and leiomyosarcoma on T2WI [19, 34]. The combination of multiple MRI sequences such as T2WI, DWI, and DCE had been proved to provide complementary information for the characterization of tumors [33]. Namimoto et al. also reported that the decrease of ADC values was associated with uterine sarcomas and combination of DWI and T2WI was able to differentiate uterine sarcomas and leiomyomas without any overlap [7]. One of the advantages of MP-MRI is the ability to combine functional and anatomical information. Therefore, better diagnostic performance of MP-MRI-based radiomics is expected in future experiments. As radiomic models will be further progressed and validated by larger clinical patient datasets at multiple institutions, it would significantly improve the preoperative diagnostic performance in distinguishing uterine sarcoma from atypical leiomyoma, thereby facilitating a more personalized approach in the management of gynecological tumors.

Our study had several limitations. First, the number of patients with uterine sarcoma included in this study was rather limited. We cannot afford to separate the data into a training set and a testing set. Furthermore, external validation sets are needed to testify the efficacy of radiomic model. Second, the variability in manual segmentation can introduce bias in the evaluation of derived radiomic features. Manual delineation is also time-consuming. Automatic and semi-automatic methods over manual contouring were recommended in radiomics [35]. Most uterus with sarcoma or atypical leiomyoma is heterogenous in density and shape which made automatic segmentation algorithms very hard to fit in well. With the development of image segmentation technology, automatic segmentation of irregular tumor or organ will be applied in future studies thus facilitating a more reproducible radiomic analysis. Third, we only used ADC maps for radiomic analyses. We anticipate that the performance of radiomic models may approve with the inclusion of MP-MRI-based radiomic features. Fourth, this study suffered from lack of standardization of DWI protocols across different scanners. Though ADC map-based features described the distribution of intensities and spatial relations between voxels which are independent of signal intensity [8], the influence of different magnetic-field-strength, sequence parameters, and artifacts cannot be neglected. Uniform acquisition parameters across scanners and institutions are needed to guarantee the reproducibility of radiomics. Finally, whole amount pathology maps correlated with MRI segmentation were not available in this study.

Conclusions

Radiomic model based on features extracted from VOI that covered the whole uterus had the best diagnostic performance in the differentiation of uterine sarcoma from leiomyoma. VOI that contained more image information was useful in improving diagnostic performance of radiomic model. However, a validation of this study in a larger, preferably multiple-center cohort with multiple MRI sequences should be pursued.

Acknowledgements. The authors of this manuscript declare no relationships with any companies, or receive any fund.

Compliance with Ethical Standards

Conflict of Interest

The authors declare that they have no conflict of interest.

Ethical Approval

All procedures performed in studies involving human participants were in accordance with the ethical standards of the institutional and with the 1964 Helsinki declaration and its later amendments. For this type of study, formal consent is not required.

References

1. Gadducci A, Cosio S, Romanini A, Genazzani AR (2008) The management of patients with uterine sarcoma: a debated clinical challenge. Crit Rev Oncol Hematol 65:129–142
2. Amant F, Coosemans A, Debiec-Rychter M, Timmerman D, Vergote I (2009) Clinical management of uterine sarcomas. Lancet Oncol 10:1188–1198
3. Pietzner K, Buttmann-Schweiger N, Sehouli J, Kraywinkel K (2018) Incidence patterns and survival of gynecological sarcoma in Germany: analysis of population-based Cancer registry data on 1066 women. Int J Gynecol Cancer 28:134–138
4. Owen C, Armstrong AY (2015) Clinical management of leiomyoma. Obstet Gynecol Clin N Am 42:67–85
5. Kim TH, Kim JW, Kim SY, Kim SH, Cho JY (2018) What MRI features suspect malignant pure mesenchymal uterine tumors rather than uterine leiomyoma with cystic degeneration? J Gynecol Oncol 29:e26
6. Guo-Fu Z, He Z, Xiao-Mei T, Hao Z (2014) Magnetic resonance and diffusion-weighted imaging in categorization of uterine sarcomas: correlation with pathological findings. Clin Imaging 38:836–844
7. Namimoto T, Yamashita Y, Awai K, Nakaura T, Yanaga Y, Hirai T, Saito T, Katabuchi H (2009) Combined use of T2-weighted and diffusion-weighted 3-T MR imaging for differentiating uterine sarcomas from benign leiomyomas. Eur Radiol 19:2756–2764
8. de Leon AD, Kapur P, Pedrosa I (2019) Radiomics in kidney Cancer: MR imaging. Magn Reson Imaging Clin N Am 27:1–13

9. Lambin P, Leijenaar RTH, Deist TM, Peerlings J, de Jong EEC, van Timmeren J, Sanduleanu S, Larue RTHM, Even AJG, Jochems A, van Wijk Y, Woodruff H, van Soest J, Lustberg T, Roelofs E, van Elmpt W, Dekker A, Mottaghy FM, Wildberger JE, Walsh S (2017) Radiomics: the bridge between medical imaging and personalized medicine. Nat Rev Clin Oncol 14:749–762
10. Lambin P, Rios-Velazquez E, Leijenaar R, Carvalho S, van Stiphout RGPM, Granton P, Zegers CML, Gillies R, Boellard R, Dekker A, Aerts HJWL (2012) Radiomics: extracting more information from medical images using advanced feature analysis. Eur J Cancer 48:441–446
11. Gillies RJ, Kinahan PE, Hricak H (2016) Radiomics: images are more than pictures, they are data. Radiology 278:563–577
12. Gevaert O, Mitchell LA, Achrol AS, Xu J, Echegaray S, Steinberg GK, Cheshier SH, Napel S, Zaharchuk G, Plevritis SK (2014) Glioblastoma multiforme: exploratory radiogenomic analysis by using quantitative image features. Radiology 273:168–174
13. Prasanna P, Patel J, Partovi S, Madabhushi A, Tiwari P (2017) Radiomic features from the peritumoral brain parenchyma on treatment-naive multi-parametric MR imaging predict long versus short-term survival in glioblastoma multiforme: preliminary findings. Eur Radiol 27:4188–4197
14. Shen C, Liu Z, Guan M, Song J, Lian Y, Wang S, Tang Z, Dong D, Kong L, Wang M, Shi D, Tian J (2017) 2D and 3D CT Radiomics features prognostic performance comparison in non-small cell lung Cancer. Transl Oncol 10:886–894
15. Li H, Zhu Y, Burnside ES, Drukker K, Hoadley KA, Fan C, Conzen SD, Whitman GJ, Sutton EJ, Net JM, Ganott M, Huang E, Morris EA, Perou CM, Ji Y, Giger ML (2016) MR imaging Radiomics signatures for predicting the risk of breast Cancer recurrence as given by research versions of MammaPrint, Oncotype DX, and PAM50 gene assays. Radiology 281:382–391
16. Wibmer A, Hricak H, Gondo T, Matsumoto K, Veeraraghavan H, Fehr D, Zheng J, Goldman D, Moskowitz C, Fine SW, Reuter VE, Eastham J, Sala E, Vargas HA (2015) Haralick texture analysis of prostate MRI: utility for differentiating non-cancerous prostate from prostate cancer and differentiating prostate cancers with different Gleason scores. Eur Radiol 25:2840–2850
17. Lerski RA, Straughan K, Schad LR, Boyce D, Bluml S, Zuna I (1993) MR image texture analysis–an approach to tissue characterization. Magn Reson Imaging 11:873–887
18. Kotrotsou A, Zinn PO, Colen RR (2016) Radiomics in brain tumors: An Emerging Technique for Characterization of Tumor Environment. Magn Reson Imaging 24:719–729
19. Lakhman Y, Veeraraghavan H, Chaim J, Feier D, Goldman DA, Moskowitz CS, Nougaret S, Sosa RE, Vargas HA, Soslow RA, Abu-Rustum NR, Hricak H, Sala E (2017) Differentiation of uterine Leiomyosarcoma from atypical leiomyoma: diagnostic accuracy of qualitative MR imaging features and feasibility of texture analysis. Eur Radiol 27:2903–2915
20. Kumar V, Gu Y, Basu S, Berglund A, Eschrich SA, Schabath MB, Forster K, Aerts HJWL, Dekker A, Fenstermacher D, Goldgof DB, Hall LO, Lambin P, Balagurunathan Y, Gatenby RA, Gillies RJ (2012) Radiomics: the process and the challenges. Magn Reson Imaging 30:1234–1248
21. Kotrotsou A, Zinn P, Colen R (2015) Introduction to texture analysis for brain tumors: concept and clinical relevance [abstract]. American Society of Neuroradiology 53rd Annual Meeting
22. Tanos V, Berry KE (2018) Benign and malignant pathology of the uterus. Best Pract Res Clin Obstet Gynaecol 46:12–30
23. Sahdev A, Sohaib SA, Jacobs I, Shepherd JH, Oram DH, Reznek RH (2001) MR imaging of uterine sarcomas. AJR Am J Roentgenol 177:1307–1311
24. Bi Q, Xiao Z, Lv F, Liu Y, Zou C, Shen Y (2018) Utility of clinical parameters and multiparametric MRI as predictive factors for differentiating uterine sarcoma from atypical leiomyoma. Acad Radiol 25:993–1002
25. Vallieres M, Freeman CR, Skamene SR, El Naqa I (2015) A radiomics model from joint FDG-PET and MRI texture features for the prediction of lung metastases in soft-tissue sarcomas of the extremities. Phys Med Biol 60:5471–5496
26. Zhou H, Vallieres M, Bai HX et al (2017) MRI features predict survival and molecular markers in diffuse lower-grade gliomas. Neuro-Oncology 19:862–870
27. Dong Y, Feng Q, Yang W, Lu Z, Deng C, Zhang L, Lian Z, Liu J, Luo X, Pei S, Mo X, Huang W, Liang C, Zhang B, Zhang S (2018) Preoperative prediction of sentinel lymph node metastasis in breast cancer based on radiomics of T2-weighted fat-suppression and diffusion-weighted MRI. Eur Radiol 28:582–591
28. Zou KH, Warfield SK, Bharatha A, Tempany CMC, Kaus MR, Haker SJ, Wells WM III, Jolesz FA, Kikinis R (2004) Statistical validation of image segmentation quality based on a spatial overlap index. Acad Radiol 11:178–189
29. Chen Y, Chen TW, Wu CQ, Lin Q, Hu R, Xie CL, Zuo HD, Wu JL, Mu QW, Fu QS, Yang GQ, Zhang XM (2018) Radiomics model of contrast-enhanced computed tomography for predicting the recurrence of acute pancreatitis. Eur Radiol. https://doi.org/10.1007/s00330-018-5824-1
30. Tanadini-Lang S, Bogowicz M, Veit-Haibach P, Huellner M, Pauli C, Shukla V, Guckenberger M, Riesterer O (2018) Exploratory Radiomics in computed tomography perfusion of prostate Cancer. Anticancer Res 38:685–690
31. Nekooeimehr I, Lai-Yuen S, Bao P et al (2016) Automated tracking, segmentation and trajectory classification of pelvic organs on dynamic MRI. Conf Proc IEEE Eng Med Biol Soc 2016:2403–2406
32. Colen R, Hatami M, Kotrotsou A et al (2015) NIMG-11: radiomic subclassification of glioblastoma. Neuro Oncol 17:v155–v155
33. Malayeri AA, El Khouli RH, Zaheer A et al (2011) Principles and applications of diffusion-weighted imaging in cancer detection, staging, and treatment follow-up. Radiographics 31:1773–1791
34. Gerges L, Popiolek D, Rosenkrantz AB (2018) Explorative investigation of whole-lesion histogram MRI metrics for differentiating uterine leiomyomas and Leiomyosarcomas. AJR Am J Roentgenol 210:1172–1177
35. Yip SS, Aerts HJ (2016) Applications and limitations of radiomics. Phys Med Biol 61:R150–R166